Available online at www.sciencedirect.com
ScienceDirect
Journal of Organometallic Chemistry 692 (2007) 4481–4485
Journal of Organometallic Chemistry
www.elsevier.com/locate/jorganchem

Reactions of the titanium-carbide species $CpTi(\mu^2\text{-}Me)(\mu^2\text{-}NPi\text{-}Pr_3)(\mu^4\text{-}C)(AlMe_2)_3$

Todd W. Graham, Christopher Ong, Pingrong Wei, Douglas W. Stephan *

University of Windsor, Chemistry and Biochemistry, 401 Sunset Ave, Windsor, ON, Canada N9B3P4

Received 7 February 2007; received in revised form 5 March 2007; accepted 6 March 2007
Available online 16 March 2007

Dedicated to a friend and a scholar, Gerhard Erker, on the occasion of his 60th birthday.

Abstract

The reaction of $CpTi(\mu^2\text{-}Me)(\mu^2\text{-}NPi\text{-}Pr_3)(\mu^4\text{-}C)(AlMe_2)_3$ with $ClSnMe_3$ and MeO_3SCF_3 affords the species $CpTi(\mu^2\text{-}Cl)(\mu^2\text{-}NPi\text{-}Pr_3)(\mu^4\text{-}C)(\mu^2\text{-}Cl)(AlMe)(AlMe_2)_2$ **1** and $CpTi(\mu^2\text{-}Me)(\mu^2\text{-}NPi\text{-}Pr_3)(\mu^4\text{-}C)(\mu^2\text{-}O_3SCF_3)(AlMe)(AlMe_2)_2$ **2**, respectively. Both **1** and **2** have been structurally characterized.

Keywords: Carbide; Titanium; Aluminum; Crystal structure

1. Introduction

C–H bond activation has and continues to be of widespread interest to the chemical community. Since the early 1980s [1,2], a variety of approaches to C–H activation have been examined [3–8]. In the 1990s and into the current decade the research groups of Smith [9–14] and Hartwig [15–25] among others have developed a range of catalysts that utilize C–H bond activation to effect functionalization of alkanes. Our interest in C–H bond activation lies in the potential to generate unusual transition metal derivatives. In our own work we have recently described the reactions of Ti and Zr-phosphinimide complexes with the Lewis acid $AlMe_3$ [26,27]. that lead to multiple C–H activation processes. For example, reactions of $CpM(NPR_3)Me_2$ (M = Ti, Zr) with excess $AlMe_3$, result in the formation of the Ti-carbide species $CpTi(\mu^2\text{-}Me)(\mu^2\text{-}NPR_3)(\mu^4\text{-}C)(AlMe_2)_3$ (**a**), or $CpTi(\mu^2\text{-}Me)(\mu^2\text{-}NPR_3)(\mu^5\text{-}C)(AlMe_2)_3\cdot(AlMe_3)$ [26,27] (**b**) and the Zr-methanide derivatives, $(Cp^*Zr)_4(\mu\text{-}Cl)_5(Cl)(\mu\text{-}CH)_2$ and $(Cp^*Zr)_5(\mu\text{-}Cl)_6(\mu\text{-}CH)_3$ [28]. Additionally, we have published the mechanistic details of the divergent C–H activation pathways observed in the reaction of $(t\text{-}Bu_3PN)_2TiMe_2$ with $AlMe_3$, which affords $[(\mu^2\text{-}t\text{-}Bu_3PN)Ti(\mu\text{-}Me)(\mu^4\text{-}C)(AlMe_2)_2]_2$ (**c**) and $(t\text{-}Bu_3PN)Ti(\mu^2\text{-}t\text{-}Bu_3PN)(\mu^3\text{-}CH_2)_2(AlMe_2)_2(AlMe_3)$ (**d**) [29]. Related C–H activations in the formation of the Zr and Hf clusters, $(Cp^*M)_3Al_6Me_8(\mu^3\text{-}CH_2)_2(\mu^4\text{-}CH)_4(\mu^3\text{-}CH)$ (M = Zr, Hf) have also been previously described by Roesky et al. [30,31]. Much of this chemistry is reminiscent of the C–H bond activation in the formation of the well-known Tebbe reagent, $Cp_2Ti(\mu\text{-}CH_2)(\mu\text{-}Cl)AlMe_2$ [32]. This similarity prompts questions regarding the reactivity of our products of multiple C–H activations. In this note, we described some reactions of the Ti-carbide species $CpTi(\mu^2\text{-}Me)(\mu^2\text{-}NP^iPr_3)(\mu^4\text{-}C)(AlMe_2)_3$. Although one might anticipate interesting reactivity at the carbide fragment these studies reveal the robust nature of the Ti-carbide fragment.

* Corresponding author.
E-mail address: stephan@uwindsor.ca (D.W. Stephan).

0022-328X/$ - see front matter © 2007 Elsevier B.V. All rights reserved.
doi:10.1016/j.jorganchem.2007.03.011

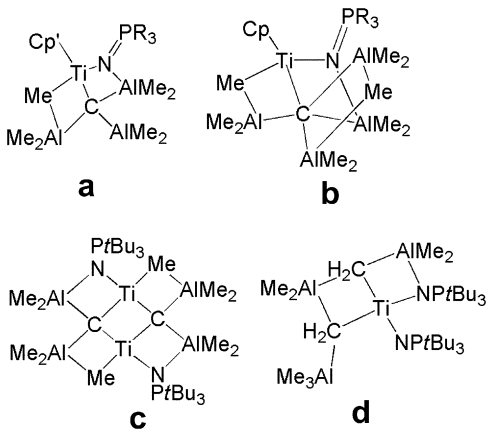

2. Experimental

2.1. General data

All preparations were done under an atmosphere of dry, O_2-free N_2 employing both Schlenk line techniques and a Vacuum Atmospheres inert atmosphere glove box. Solvents were purified employing a Grubbs' type solvent purification system manufactured by Innovative Technology. All organic reagents were purified by conventional methods. ^{1}H NMR spectra were recorded on Bruker Avance-300 and 500 spectrometers. All spectra were recorded in C_6D_6 at 25 °C unless otherwise noted. Trace amounts of protonated solvents were used as references and chemical shifts are reported relative to $SiMe_4$. $^{31}P\{^1H\}$ NMR spectra were recorded on a Bruker Avance-300 and are referenced to external 85% H_3PO_4. Combustion analyses were done in house employing a Perkin Elmer CHN Analyzer. CpTi(μ^2-Me)(μ^2-NP*i*-Pr$_3$)(μ^4-C)(AlMe$_2$)$_3$ was prepared as previously described [26,27].

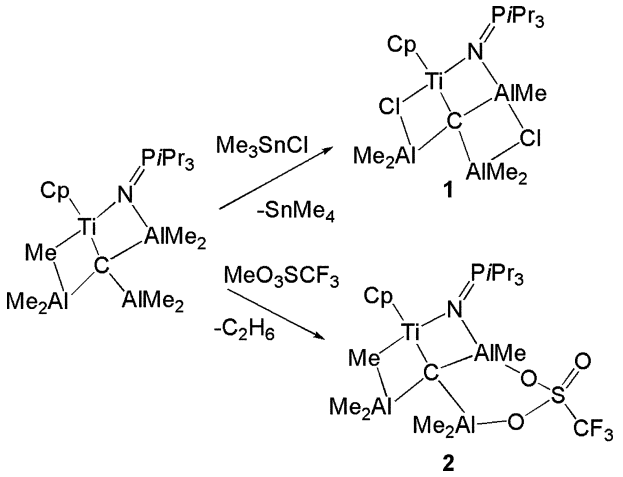

Scheme 1.

2.2. Synthesis of CpTi(μ^2-Cl)(μ^2-NPi-Pr$_3$)(μ^4-C)-(μ^2-Cl)(AlMe)(AlMe$_2$)$_2$ 1

$ClSnMe_3$ (0.038 g; 0.194 mmol) was added to a solution of CpTi(μ^2-Me)(μ^2-NP*i*-Pr$_3$)(μ^4-C)(AlMe$_2$)$_3$ (0.047 g; 0.097 mmol) in C_6H_6. The reaction mixture was allowed to stir for 12 h and the solvent was then removed under vacuum. Recrystallization from benzene (1 mL) at 25 °C afforded **1** as yellow crystals. Yield: 67%. ^{1}H NMR δ: 6.40 (s, 5H, Cp), 1.86 (m, 3H, CH), 0.84 (m, 18H, Me), 0.12 (s, 3H, AlMe) 0.07 (s, 6H, AlMe), −0.08 (s, 6H, AlMe). $^{31}P\{^1H\}$ NMR δ: 53.8. Anal. Calc. for $C_{20}H_{41}Al_3Cl_2NPTi$: C, 45.65; H, 7.85; N, 2.66. Found: C, 45.35; H, 7.47; N, 2.29% (Scheme 1).

2.3. Synthesis of CpTi(μ^2-Me)(μ^2- NPi-Pr$_3$)(μ^4-C)-(μ^2-O$_3$SCF$_3$)(AlMe)(AlMe$_2$)$_2$ 2

MeO_3SCF_3 (35 μL, 0.309 mmol, 1.5 equiv.) was added to a solution of CpTi(μ^2-Me)(μ^2-NPiPr$_3$)(μ^4-C)(AlMe$_2$)$_3$-(μ^2-MeAlMe$_2$) (100 mg, 0.206 mmol) in 3 mL of benzene and the mixture stirred overnight. The solvent was removed *in vacuo* and the residue was then washed with pentane and dried *in vacuo*. Yield: 70 %. Recrystallization from benzene (1 mL) at 25 °C afforded crystals of **2**. ^{1}H NMR δ: 6.26 (s, 5H Cp); 1.63 (sept, $^3J_{HH} = 7$ Hz; 3H, CH); 0.69 (dd, $^3J_{HH} = 7$ Hz, $^3J_{PH} = 15$ Hz, *i*-Pr); 0.57 (dd, $^3J_{HH} = 7$ Hz, $^3J_{PH} = 15$ Hz, Me); 0.20 (s, 3H, AlMe); 0.14 (s, 3H AlMe); 0.00 (s, 3H, AlMe); −0.06 (s, 3H, AlMe); −0.14 (s, 3H, μ-Me). $^{31}P\{^1H\}$ NMR δ: 54.2 (s). Anal. Calc. for $C_{22}H_{44}F_3Al_3NO_3PSTi$: C, 42.65; H, 7.16; N, 2.26. Found: C, 42.25; H, 7.00; N, 2.03%.

2.4. X-ray data collection and reduction

Crystals were manipulated and mounted in capillaries in a glove box, thus maintaining a dry, O_2-free environment for each crystal. Diffraction experiments were performed on a Siemens SMART System CCD diffractometer. The data were collected in a hemisphere of data in 1329 frames with 10 s exposure times. The observed extinctions were consistent with the space groups in each case. The data sets were collected ($4.5° < 2\theta < 45$–$50.0°$). A measure of decay was obtained by re-collecting the first 50 frames of each data set. The intensities of reflections within these frames showed no statistically significant change over the duration of the data collections. The data were processed using the SAINT and XPREP processing packages. An empirical absorption correction based on redundant data was applied to each data set. Subsequent solution and refinement was performed using the SHELXTL solution package (Table 1).

2.5. Structure solution and refinement

Non-hydrogen atomic scattering factors were taken from the literature tabulations [33]. The heavy atom positions were determined using direct methods employing

Table 1
Crystallographic data

	1	2
Formula	$C_{20}H_{41}Al_3Cl_2NPTi$	$C_{22}H_{44}Al_3F_3NO_3PSTi$
Formula weight	526.25	619.45
a (Å)	9.9960(1)	10.936(7)
b (Å)	19.2650(1)	16.308(12)
c (Å)	15.234(2)	19.293(14)
β (°)	93.556(10)	102.671(14)
Crystal system	Monoclinic	Monoclinic
V (Å^3)	2928.24(4)	3357(4)
Space group	$P2_1/n$	$P2_1/n$
d(calc) (g cm^{-1})	1.194	1.226
Z	4	4
Absorption coefficient, μ (cm^{-1})	0.627	0.482
Data collected	8943	13998
Data $F_o^2 > 3\sigma(F_o^2)$	3113	4746
Variables	253	316
R	0.1100	0.0484
R_w	0.3007	0.1413
GOF	1.212	1.021

$R = \sum\|F_o| - |F_c\|/\sum|F_o|$, $R_w = [\sum[\omega(F_o^2 - F_c^2)^2]/\sum[\omega(F_o^2)^2]]^{0.5}$.

the SHELXTL direct methods routine. The remaining non-hydrogen atoms were located from successive difference Fourier map calculations. The refinements were carried out by using full-matrix least squares techniques on F^2, minimizing the function $\omega\ (|F_o| - |F_c|)^2$ where the weight ω is defined as $4F_o^2/2\sigma(F_o^2)$ and F_o and F_c are the observed and calculated structure factor amplitudes. In the final cycles of each refinement, all non-hydrogen atoms were assigned anisotropic temperature factors in the absence of disorder or insufficient data. In the latter cases atoms were treated isotropically. C–H atom positions were calculated and allowed to ride on the carbon to which they are bonded assuming a C–H bond length of 0.95 Å. H-atom temperature factors were fixed at 1.10 times the isotropic temperature factor of the C-atom to which they are bonded. The H-atom contributions were calculated, but not refined. The locations of the largest peaks in the final difference Fourier map calculation as well as the magnitude of the residual electron densities in each case were of no chemical significance. Addition details are provided in the Supplementary material.

3. Results and discussion

The Ti-carbide species CpTi(μ^2-Me)(μ^2-NP*i*-Pr$_3$)-(μ^4-C)(AlMe$_2$)$_3$ was prepared as was previously described [26,27], and we have now explored reactions of this species with a variety of reagents. Few of these efforts yielded new products, and in no case was there evidence of reaction at the carbide carbon. We have previously described reactions with thiols [34], however, polar reagents were much less reactive in general. Nonetheless, reaction with Me$_3$SnCl did give a new product **1** as evidence by ^{31}P NMR spectroscopy. The ^{1}H NMR spectra were consistent with the presence of three types of methyl groups in a 1:2:2 ratio. Notably, these resonances were broad, consistent with Al-bound methyl groups. Low temperature NMR experiments failed to further resolve these signals, consistent with the possibility of low-energy methyl-group exchange processes. Recrystallization of **1** afforded relatively poor X-ray quality crystals. Nonetheless, the structural determination revealed the connectivity and affirmed the formulation of **1** as CpTi(μ^2-Cl)(μ^2-NP*i*-Pr$_3$)(μ^4-C)(μ^2-Cl)(AlMe)-(AlMe$_2$)$_2$ (Scheme 1, Fig. 1).

The geometry of **1** is reminiscent of CpTi(μ^2-Me)-(μ^2-NP*i*-Pr$_3$)(μ^4-C)(AlMe$_2$)$_3$, with the Ti center adopting a pseudo "three-legged piano stool" coordination sphere comprised of a cyclopentadienyl a chloride, a phosphinimide nitrogen atom, and a carbide carbon atom. The carbide carbon is also coordinated to three aluminum atoms. Two AlMe$_2$ moieties (Al(1), Al(2)) bridge the titanium and aluminum bound chloride atoms, while a third Al atom, Al(3), on the carbide carbon atom bridges to the Ti via the phosphinimide nitrogen and to Al(2) via chloride. The Ti–Cl distance was found to be 2.406(4) Å while the Al–Cl distances are 2.403(5) Å and 2.308(5) Å. The geometries about the Al atoms are pseudo-tetrahedral while the carbide carbon atom (C(15)) adopts a somewhat distorted tetrahedral geometry. This is reflected in the variations in the angles about Al as the Ti(1)–C(15)–Al(2) is flattened to 141.7(6)° and the Ti(1)–C(15)–Al(3) is clearly more strained at 87.6(5)°. The Ti–C distance to the carbide carbon is 1.851(12) Å and is shorter than that reported for CpTi(μ^2-Me)(μ^2-NP*i*-Pr$_3$)(μ^4-C)(AlMe$_2$)$_3$ (1.891(6) Å) and

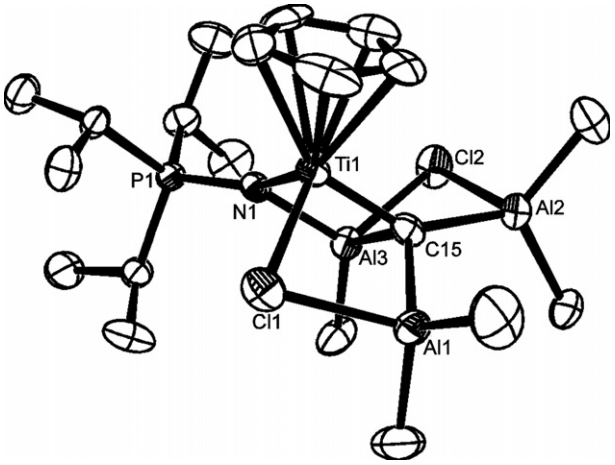

Fig. 1. ORTEP drawing of **1**, 30% thermal ellipsoids are shown. Hydrogen atoms are omitted for clarity. Distances (Å) angles (°): Ti(1)–C(15) 1.851(12), Ti(1)–N(1) 1.988(9), Ti(1)–Cl(1) 2.406(4), Al(1)–C(15) 1.990(12), Al(1)–Cl(1) 2.403(5), Al(2)–C(15) 2.009(12), Al(3)–N(1) 1.870(9), Al(3)–C(15) 1.985(11), Al(3)–Cl(2) 2.308(5), P(1)–N(1) 1.610(9), C(15)–Ti(1)–N(1) 93.0(4), C(15)–Ti(1)–Cl(1) 93.9(4), N(1)–Ti(1)–Cl(1) 106.9(3), C(15)–Al(1)–Cl(1) 90.5(4), C(15)–Al(2)–Cl(2) 87.4(4), N(1)–Al(3)–C(15) 92.5(5), Al(1)–Cl(1)–Ti(1) 74.54(13), Al(3)–Cl(2)–Al(2) 75.64(15), P(1)–N(1)–Al(3) 130.7(5), P(1)–N(1)–Ti(1) 141.5(5), Al(3)–N(1)–Ti(1) 87.0(4), Ti(1)–C(15)–Al(3) 87.6(5), Ti(1)–C(15)–Al(1) 98.6(5), Al(3)–C(15)–Al(1) 120.3(6), Ti(1)–C(15)–Al(2) 141.7(6), Al(3)–C(15)–Al(2) 94.1(5), Al(1)–C(15)–Al(2) 113.1(6).

$CpTi(\mu^2\text{-}Me)(\mu^2\text{-}NPR_3)(\mu^5\text{-}C)(AlMe_2)_3 \cdot (AlMe_3)$ (1.878(4) Å) [26,27]. In contrast, the carbide-C–Al distances in **1** are slightly longer (1.990(12) Å, 2.009(12) Å, 1.985(11) Å) compared to those in than those in $CpTi(\mu^2\text{-}Me)(\mu^2\text{-}NPi\text{-}Pr_3)(\mu^4\text{-}C)(AlMe_2)_3$ (1.974(6) Å) [26,27]. This presumably reflects donation of electron density from the chlorides to the Al atoms which increases the relative acidity of the Ti center, thus shortening the Ti–C bond. As well, this donation is reflected in the slightly shorter Ti–N distance of 1.988(9) Å and the Al–N distance of 1.870(9) Å.

In a similar and related reaction, the Ti-carbide species $CpTi(\mu^2\text{-}Me)(\mu^2\text{-}NPi\text{-}Pr_3)(\mu^4\text{-}C)(AlMe_2)_3$ reacted cleanly with MeO_3SCF_3, affording the product **2**, which exhibited a single ^{31}P resonance at 54.2 ppm. In contrast to **1**, the ^1H NMR spectra of **2** showed six well resolved methyl-resonances attributable to the Al–Me and Ti–Me groups. In addition, resonances resulting from the presence of the *i*-Pr_3P fragment were also observed (Fig. 2). These data suggest a structure in which the Al-bound methyl groups are locked in non-exchanging, markedly inequivalent environments. An X-ray structural determination revealed the formulation of **2** as $CpTi(\mu^2\text{-}Me)(\mu^2\text{-}NPi\text{-}Pr_3)(\mu^4\text{-}C)(\mu^2\text{-}O_3SCF_3)(AlMe)(AlMe_2)_2$ (Fig. 3). The overall geometry of **2** is somewhat similar to those of both **1** and $CpTi(\mu^2\text{-}Me)(\mu^2\text{-}NPi\text{-}Pr_3)(\mu^4\text{-}C)(AlMe_2)_3$ [26,27]. Compound **2** contains a triflate group that bridges two of the carbide-bound Al atoms similar to one of the Cl-atoms in **1**. At the same time, a methyl group bridge is apparent between Al and Ti, similar to $CpTi(\mu^2\text{-}Me)(\mu^2\text{-}NPi\text{-}Pr_3)(\mu^4\text{-}C)(AlMe_2)_3$ [26,27]. The metric parameters about the Ti, carbide and Al atoms reflect these comparisons as well. The Ti(1)–C(1) and Ti–N distance of 1.901(4) Å and 2.011(3) Å, respectively, are slightly longer than those observed in **1**, as is the Al–N distance of 1.881(3) Å. This reflects the presence of the electron donating methyl group in place of Cl. The bridging methyl Ti–C(2) distance is 2.359(4) Å. The geometry about the carbide carbon is also distorted in **2** with a Ti(1)–C(1)–Al(2) angle of 145.0(2)° while the Ti(1)–C(1)–Al(1) is constrained to 86.32(14)° as a result of the TiNCAl four-membered ring. The triflate group bridges Al(1) and Al(2) forming a six-membered ring with Al–O distances of 1.916(3) Å and 1.983(4) Å, respectively. This CAl_2O_2S ring adopts a pseudo-boat conformation placing the sterically demanding CF_3 group in a pseudo-axial position. The bridging S–O distances were found to be 1.437(4) Å and 1.462(3) Å, respectively while the terminal S–O distance is shorter (1.405(4) Å) as expected.

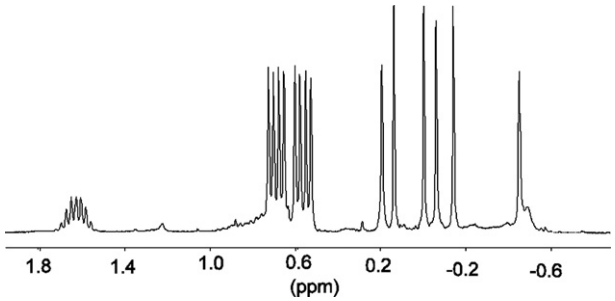

Fig. 2. Methyl and methine region of the ^1H NMR spectrum of **2**.

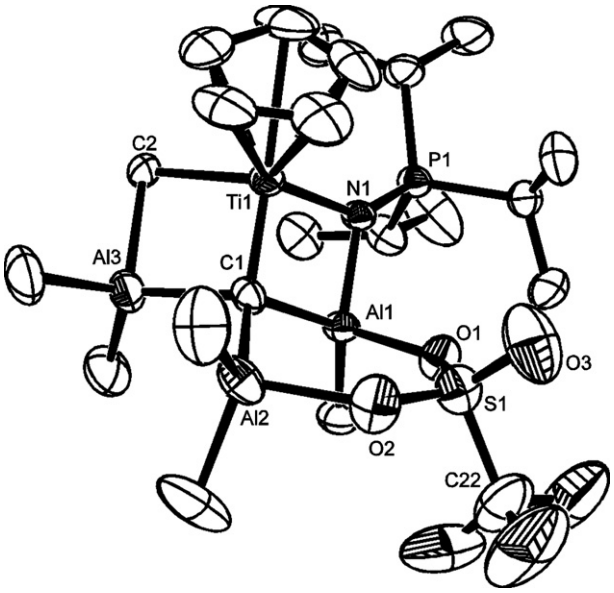

Fig. 3. ORTEP drawing of **2**, 30% thermal ellipsoids are shown. Hydrogen atoms are omitted for clarity. Distances (Å) angles (°): Ti(1)–C(1) 1.901(4), Ti(1)–N(1) 2.011(3), Ti(1)–C(2) 2.359(4), Al(1)–N(1) 1.881(3), Al(1)–O1 1.916(3), Al(1)–C(1) 1.999(4), Al(2)–O2 1.983(4), Al(2)–C(1) 1.988(4), Al(3)–C(1) 2.037(4), Al(3)–C(2) 2.221(4), P(1)–N(1) 1.612(3), S(1)–O(3) 1.405(4), S(1)–O(2) 1.437(4), S(1)–O(1) 1.462(3), C(1)Ti(1)–N(1) 93.10(13), C(1)Ti(1)-C12 95.7(2), N(1)–Ti(1)–C12 113.4(2), C(1)Ti(1)–C(2) 97.06(15), N(1)–Ti(1)–C(2) 106.39(14), N(1)–Al(1)–O(1) 106.19(14), N(1)–Al(1)–C(1) 94.08(14), O(1)–Al(1)–C(1) 103.33(15), O(2)–Al(2)–C(1) 101.37(15), C(1)Al(3)–C(2) 97.62(16), O(3)–S(1)–O(2) 116.2(3), O(3)–S(1)–O(1) 114.9(3), O(2)–S(1)–O(1) 112.54(19), O(3)–S(1)–C(22) 103.8(4), O(2)–S(1)–C(22) 104.9(3), O(1)–S(1)–C(2)2 102.4(3), S(1)–O(1)–Al(1) 136.3(2), S(1)–O(2)–Al(2) 137.9(2), P(1)–N(1)–Al(1) 130.88(17), P(1)–N(1)–Ti(1) 142.35(18), Al(1)–N(1)–Ti(1) 86.49(12), Ti(1)–C(1)–Al(2) 145.0(2), Ti(1)–C(1)–Al(1) 86.32(14), Al(2)–C(1)–Al(1) 113.02(19), Ti(1)–C(1)–Al(3) 89.41(17), Al(2)–C(1)–Al(3) 106.01(17), Al(1)–C(1)–Al(3) 115.80(18), Al(3)–C(2)–Ti(1) 74.41(13).

The characterization of **1** and **2** illustrates that the reactivity of $CpTi(\mu^2\text{-}Me)(\mu^2\text{-}NPi\text{-}Pr_3)(\mu^4\text{-}C)(AlMe_2)_3$ is dominated by the Lewis acidity of the three coordinate Al center and subsequently at the methyl group bridging Ti and Al. It is reasonable to speculate that in the case of Me_3SnCl, initial interaction with Al affords methyl for Cl exchange generating $SnMe_4$. Subsequent functionality could lead to exchange of the Cl into the Ti, Al bridging site to give **1**. In the case of the formation of **2**, as elimination of ethane from a metal-methyl group and MeO_3SCF_3 is unprecedented, it is most likely that MeO_3SCF_3 reacts with adventious water generating HO_3SCF_3. Subsequent reaction with an AlMe bond liberates methane and yields the six-membered chelate ring incorporating the two Al centers in **2**.

Thus in summary while it is true early metal–carbon bonds are generally reactive, the chemistry described herein and elsewhere [26,27] affirms that the reactivity of CpTi-

$(\mu^2\text{-Me})(\mu^2\text{-NP}i\text{-Pr}_3)(\mu^4\text{-C})(\text{AlMe}_2)_3$ occurs on the periphery of the molecule. This demonstrates the robust nature and stability of the $TiCAl_3$ core of these $TiAl_3$-carbide species.

Acknowledgments

Financial support from NSERC of Canada and NOVA Chemicals Corporation is gratefully acknowledged.

Appendix A. Supplementary material

CCDC 636038 and 636039 contain the supplementary crystallographic data for **1** and **2**. The data can be obtained free of charge via http://www.ccdc.cam.ac.uk/conts/retrieving.html, or from the Cambridge Crystallographic Data Centre, 12 Union Road, Cambridge CB2 1EZ, UK; fax: (+44) 1223-336-033; or e-mail: deposit@ccdc.cam.ac.uk. Supplementary data associated with this article can be found, in the online version, at doi:10.1016/j.jorganchem.2007.03.011.

References

[1] J. Hoyano, W.A. Graham, J. Am. Chem. Soc. 104 (1982) 3723.
[2] A.H. Janowicz, R.G. Bergman, J. Am. Chem. Soc. 105 (1983) 3929–3939.
[3] A.S. Goldman, K.I. Goldberg, ACS Symp. Ser. 885 (2004) 1–43.
[4] J.A. Labinger, J.E. Bercaw, Nature 417 (2002) 507–514.
[5] Y. Fujiwara, C. Jia, Pure Appl. Chem. 73 (2001) 319–324.
[6] B.A. Arndtsen, R.G. Bergman, J.A. Mobley, T.H. Peterson, Acc. Chem. Res. 28 (1995) 154–162.
[7] R.H. Crabtree, in: R.H. Crabtree, S. Patai, Z. Rappoprt (Eds.), The Organometallic Chemistry of the Transition Metals, John Wiley & Sons, New York, 1992, p. 653.
[8] R.H. Crabtree, Chem. Rev. 95 (1995) 987.
[9] F. Shi, R. Smith Milton 3rd., E. Maleczka Robert Jr., Org. Lett. 8 (2006) 1411–1414.
[10] A. Chotana Ghayoor, A. Rak Michael, R. Smith Milton 3rd., J. Am. Chem. Soc. 127 (2005) 10539–10544.
[11] E. Maleczka Robert Jr., F. Shi, D. Holmes, R. Smith Milton 3rd., J. Am. Chem. Soc. 125 (2003) 7792–7793.
[12] J.-Y. Cho, K. Tse Man, D. Holmes, E. Maleczka Robert Jr., R. Smith Milton 3rd., Science 295 (2002) 305–308.
[13] B. Qian, W.J. Scanlon, M.R. Smith III., D.H. Motry, Organometallics 18 (1999) 1693–1698.
[14] C.N. Iverson, M.R. Smith III., J. Am. Chem. Soc. 121 (1999) 7696–7697.
[15] J.F. Hartwig, R.A. Andersen, R.G. Bergman, J. Am. Chem. Soc. 113 (1991) 6492–6498.
[16] J.F. Hartwig, X. He, Angew. Chem., Int. Ed. Engl. 35 (1996) 315–317.
[17] J.F. Hartwig, Angew. Chem., Int. Ed. 37 (1998) 2046–2067.
[18] M. Kawatsura, J.F. Hartwig, J. Am. Chem. Soc. 121 (1999) 1473–1478.
[19] K.M. Waltz, C.N. Muhoro, J.F. Hartwig, Organometallics 18 (1999) 3383–3393.
[20] T. Ishiyama, J. Takagi, Y. Yonekawa, J.F. Hartwig, N. Miyaura, Adv. Synth. Catal. 345 (2003) 1103–1106.
[21] M. Kanzelberger, X. Zhang, T.J. Emge, A.S. Goldman, J. Zhao, C. Incarvito, J.F. Hartwig, J. Am. Chem. Soc. 125 (2003) 13644–13645.
[22] C.E. Webster, Y. Fan, M.B. Hall, D. Kunz, J.F. Hartwig, J. Am. Chem. Soc. 125 (2003) 858–859.
[23] M. Boller Timothy, M. Murphy Jaclyn, M. Hapke, T. Ishiyama, N. Miyaura, F. Hartwig John, J. Am. Chem. Soc. 127 (2005) 14263–14278.
[24] T.M. Boller, J.M. Murphy, M. Hapke, T. Ishiyama, N. Miyaura, J.F. Hartwig, J. Am. Chem. Soc. 127 (2005) 14263–14278.
[25] J.M. Murphy, J.D. Lawrence, K. Kawamura, C. Incarvito, J.F. Hartwig, J. Am. Chem. Soc. 128 (2006) 13684–13685.
[26] J.E. Kickham, F. Guerin, J.C. Stewart, D.W. Stephan, Angew. Chem., Int. Ed. Engl. 39 (2000) 3263–3266.
[27] J.E. Kickham, F. Guerin, J.C. Stewart, E. Urbanska, C.M. Ong, D.W. Stephan, Organometallics 20 (2001) 1175–1182.
[28] N. Yue, E. Hollink, F. Guerin, D.W. Stephan, Organometallics 20 (2001) 4424–4433.
[29] J.E. Kickham, F. Guerin, D.W. Stephan, J. Am. Chem. Soc. 124 (2002) 11486–11494.
[30] A. Herzog, H.W. Roesky, F. Jager, A. Steiner, M. Noltemeyer, Organometallics 15 (1996) 909–917.
[31] A. Herzog, H.W. Roesky, Z. Zak, M. Noltemeyer, Angew. Chem., Int. Ed. Engl. 33 (1994) 967–968.
[32] F.N. Tebbe, G.W. Parshall, G.S. Reddy, J. Am. Chem. Soc. 100 (1978) 3611–3613.
[33] D.T. Cromer, J.B. Mann, Acta Cryst. A A24 (1968) 321–324.
[34] C. Ong, J. Kickham, S. Clemens, F. Guerin, D.W. Stephan, Organometallics 21 (2002) 1646–1653.